Advances in Nano Research, *Vol. 10, No. 6 (2021) 531-538*
DOI: https://doi.org/10.12989/anr.2021.10.6.531

Effects of elastic medium on the electric potential of neural tissue by using spherical bidomain Pasternak model

Muhammad Taj[1], Mohamed A. Khadimallah[2,3], Muzamal Hussain[*4], Mohamed Elbahar[2], Muhammad Safeer[1], Sehar Asghar[4], Mohammed Mujalli[2], Amjad Qazaq[2], Monzoor Ahmad[1], Elimame Elaloui[5] and Abdelouahed Tounsi[6,7]

[1]*Department of Mathematics, University of Azad Jammu and Kashmir, Muzaffarabad, 1300, Azad Kashmir, Pakistan*
[2]*Prince Sattam Bin Abdulaziz University, College of Engineering, Al-Kharj, Saudi Arabia*
[3]*Laboratory of Systems and Applied Mechanics, Polytechnic School of Tunisia, University of Carthage, Tunis, Tunisia*
[4]*Department of Mathematics, Govt. College University Faisalabad, 38000, Faisalabad, Pakistan*
[5]*Laboratory of Materials Applications in Environment, Water and Energy LR21ES15, Faculty of Sciences, University of Gafsa, Tunisia*
[6]*YFL (Yonsei Frontier Lab), Yonsei University, Seoul, Korea*
[7]*Department of Civil and Environmental Engineering, King Fahd University of Petroleum & Minerals, 31261 Dhahran, Eastern Province, Saudi Arabia*

(*Received February 25, 2021, Revised March 2, 2021, Accepted March 2, 2021*)

Abstract. An isotropic Pasternak-Like model is considered to elaborate the behavior of electric potential of neural tissue when immersed within elastic medium. Special attention is paid to the non dimensionlization of the parameters of the surrounding elastic medium. We found that shear layer potential per unit area and is the Winkler foundation-like constant, are two constants of Pasternak-like model and they actually effect on the potential of neural tissue. It is found that elastic medium affects the potential behavior of neural tissue. Elastic medium effect on the potential behavior of neural tissue is due to the Pasternak foundation parameters. Therefore the surrounding medium affects the potential of neural tissue during its transportation of functioning.

Keywords: Pasternak-Like model; electric potential; shear layer potential per unit area; Winkler foundation-like constant; neural tissue

1. Introduction

Cell is considered as a basic unit for living tissue. Cells are specified in structurally and physically for performing multiple tasks. To execute the appropriate functions of the body, it is very essential to associate the functioning of different parts of the body to the brain (Bosch *et al.* 2003). Interaction among different body parts is maintained by neurons which comprise of its basic components; sensory, relay (inter) and motor neurons (Riemann and Lephart 2002). All cells show a current alteration through the cell membrane.

Their cell membrane can produce electrochemical impulses which travel across the membrane (Weaver 1993). The electric phenomenon which is related to muscle cells is generated during the contraction and relaxation of the cell. For the proper performance of the cell function, such as ciliated and gland cells the important factor is change in voltage through the membrane (Sembulingam and Sembulingam 2012), the same source for generation of the voltage across the membrane for both nerve cells and muscle cells. For both nerve cells and muscle cells the importance of excitation is due to the generation of impulse through the membrane. This impulse travel for both nerve and muscle cell in the same manner (Nicholls and Purves 1970). Nerve cells and muscle cells are excitable. To better understand the electrical stimulation of neural tissue, we have to determine how neural tissue responds to external stimulation (Nicholls and Purves 1970). Many researchers adopted some methods to investigate this mechanical property of neurons i.e., Core Conductance Model, Parallel-Conductance Model, Hodgkin–Huxley Membrane Model etc. Recently the bidomain model using to calculate the electric effects with the source and sink points of neural tissue (Schwartz *et al.* 2018) and this model is useful in defining mechanical behaviors of the cells.

In 2015 a detailed study was made by (Schwartz and Sadleir 2015), about the analysis of bipolar external excitation of spherical tissue by spatially opposed current source and sink point. The basic purpose of this work is to determine the electric potentials inside and outside of excitable tissue by using mathematical model and current is applied from outside. This potential related to limited volume through which the electric current is propagated. Here the motivation toward assessable understanding of the disconcentrated electrophysiology of excitable tissue is due to the occurrence of magnetic resonance electrical impedance tomography (MREIT) (Seo and Woo 2011). The contrast in MREIT-as well as in alternative MR technique, Electrical Properties Tomography (EPT) (Liu *et al.* 2015) be

*Corresponding author, Research Scholar, Ph.D.,
E-mail: muzamal45@gmail.com;
muzamalhussain@gcuf.edu.pk

ISSN: 2287-237X (Print), 2287-2388 (Online)

governed by the electrical property scattered all over the region of interest. Concisely, in a MREIT scan, current is inserted into a body is show with the pulse sequence of a MRI scanner. Jena *et al*. (2020) investigated the vibration characteristics of functionally graded porous nanobeam embedded in an elastic substrate of Winkler–Pasternak type. Classical beam theory or Euler–Bernoulli beam theory has been incorporated to address the displacement of the FG nanobeam. bi-Helmholtz type of nonlocal elasticity is being used to capture the small scale effect of the FG nanobeam. Further, the nanobeam is assumed to have porosity, distributed evenly along the thickness throughout the cross-section.

This magnetic field is due to electric current (Moon and Spencer 2013) which scattered all over the whole region, we can calculate this current through the phase component of the remodeled MR images. These images are obtained by using the phase data and it is calculated by the Laplacian of the z-component of the induced magnetic field, (Seo and Woo 2011, Lee *et al.* 2014). Sedighi *et al*. (2017) provided the static and dynamic pull-in behavior of nano-beams resting on the elastic foundation based on the nonlocal theory to capture the size effects for structures in micron and sub-micron scales. For this purpose, the governing equation of motion and the boundary conditions are driven using a variational approach. This formulation includes the influences of fringing field and intermolecular forces such as Casimir and van der Waals forces.

MREIT has previously displayed clinical assurance, e.g. lesion characterization (Ferreira 2013), but it is the chance of observing brain movement with MREIT (Sadleir *et al*. 2010) that exclusively encourages this study. MREIT, influence on the detection of neural activity, so it is very helpful for the detection of MREIT influence on active and passive tissues. For the simulation of electric current, we can construct the mathematical model of neural tissue which is dissimilar to a MREIT scan. Popov (2020) predented that in spite of the presence of adhesion at the microscopic scale, the macrosopic force of adhesion vanishes. The mechanism of vanishing macroscopic adhesion is very simple: during approach of elastic bodies, asperities are elastically deformed so strongly that after unloading they destroy the microscopic adhesive junctions. Excitable tissues are consisting of cells; the electric signals are passing through action potential due to the some particular units (FitzHugh 1969). Pavlović *et al*. (2020) studied the almost-sure and moment stability of a double nanobeam system under stochastic compressive axial loading. By means of the Lyapunov exponent and the moment Lyapunov exponent method the stochastic stability of the nano system is analyzed for different system parameters under an axial load modeled as a wideband white noise process. Some researchers briefly explained the simulation of the nerve tissue by taking its maximum and minimum threshold values, which is very compulsory to study the properties of electric simulations. This methodology has been mainly beneficial in understanding cardiac activity (Sobie *et al*. 1997). Moraveji analyzed the buckling and free vibration of fiber metal-laminated (FML) plates on a total and partial elastic foundation using the generalized differential quadrature method (GDQM). The partial foundation consists of multi-section Winkler and Pasternak type elastic foundation. Taking into consideration the first-order shear deformation theory (FSDT), FML plate is modeled and its equations of motion and boundary conditions are derived using Hamilton's principle. Hussain and Selmi (2020) employmed the wave propagation approach with the combination of Pasternak foundation equation gives birth to the shell frequency equation. Mathematically, the integral form of the Lagrange energy functional is converted into a set of three partial differential equations. A cylindrical shell is placed on the elastic foundation of Pasternak. For isotropic materials, the physical properties are same everywhere, whereas the laminated and functionally graded materials, they vary from point to point. Daikh and Zenkour (2020) refined higher order nonlocal strain gradient theory for stresses and deflections of new model of functionally graded (FG) sandwich nanoplates resting on Pasternak elastic foundation. Material properties of the FG layers are supposed to vary continuously through-the-thickness according to a power function or a sigmoid function in terms of the volume fractions of the constituents.

The bidomain model (Malmivuo and Plonsey 1995), a broad view of the cable equation (Zador *et al*. 1995), has been active in this region avoiding the individual concepts of tissue, supposing a continuity of the two regions, intra-cellular and extra-cellular, coupled by a membrane and that occupy the equivalent volume (Sepulveda *et al*. 1989). Each of these regions, having all the components instead of particular units, MR imaging furthermore essentially involves be more or less over tissues. For simplicity, we use the simple geometrical model to show the changes in these images which is obtained by MREIT for neural activity. So many authors used the bidomain equations to model the behavior of tissue and they chooses the closely resembled geometry. In circular cylindrical coordinates, (Altman and Plonsey 1990) modeled a bundle of nerves as an immeasurable cylinder in an inestimable conducting bath, studying firstly with no time influence (Altman and Plonsey 1988) and short-lived stimulation (Altman and Plonsey 1990). With the passage of time they gradually increased the reality of this model, they start from isotropic monodomain and reached at the anisotropic bidomain. After this they turn to investigate the influence of radius of tissue on stimulation and impulse transmission. Miller and Henriquez (1990) and Trayanova (1990) inspected the qualities of supposing a particular fiber vs. pack, i.e., bidomain, of fibers when modeling an immeasurable cylinder of tissue excited by whichever a disk or a line source. They presented that the individual fiber core conductor model is not an irrational estimate of the control area of a large bundle of fibers but drops its strength toward the periphery of the bundle and is completely unacceptable for small bundles. Plonsey and Barr (2007) showed in a two dimensional rectangular structure, excluding for special cases, the bidomain method to forming tissue electro-physiology is not an ordinary generalization of one-dimensional cable theory (Plonsey and Barr 1984). They establish that current passes very in a different way in

isotropic tissue paralleled to anisotropic tissue with imbalanced anisotropy ratios. Roth gave fairly accurate analytic solutions to the problem of bi-syncytia with imbalanced anisotropy ratios (Roth *et al*. 1997), with rectangular coordinates. His perturbation method elaborates expansion in a parameter well-defined over the anisotropy ratios. He measured two sources: an expanding wave front that was estimated with a step function, and a point source. Consider the example of bidomain tissue in an unchanging electric field, showing the heart by way of a sphere of anisotropic tissue with a basic of blood (Trayanova *et al*. 1993). The unchanged field meant that they could adopt azimuthal independence, leaving the problem in only a two dimension spherical coordinates r and θ. Recently some researcher used different methods for nonlinear modeling (Eltaher *et al.* 2019, Ebrahimi *et al.* 2019, Safaei *et al.* 2019, Shahsavari *et al.* 2019, Benmansour *et al.* 2019).

Our present study is encouraged by the necessity to recognize the influence on MREIT images of excitable tissue precisely, a ganglion excised from the abdomen of a sea slug exaggerated by currents injection through electrodes fixed into the boundary of its non-natural sea water bath. We cultivate a model that is a melodramatic interpretation of the real experiment but which still is unusual for its simplification in three dimensional spherical coordinate system. This model will represent elementary electrophysiological phenomena and can perform as a standard contrary to which numeric simulations such as finite element models (FEM) are held, advancing reliability to those in coincidence. This work can help as the ground work for more and more refined analytic modeling.

In this study the spherical two dimensional analysis of neural tissue, we model the Aplysia abdominal ganglion (AG), identified to be electrically attached by gap junctions (Blochlinger *et al*. 1988), in place of an isotropic bidomain sphere, the simulated sea water bath as an unbounded isotropic conducting medium and the injection currents as source as sink points. We suppose isotropic conductivity here for simplicity. For elastic medium, we will use Pasternak model, and for neural tissue, Bidomain model is used. By combining both models, we will develop spherical Bidomain Pasternak-like model. This model has been used (Taj and Zhang 2014) for wave propagation of orthotropic MTs within elastic medium and also used for vibrational behavior of embedded of MTs (Taj and Zhang 2012) with local orthotropic elastic shell model.

2. Materials and methods

Bidomain model is used to analyze the current impulse in neural tissues. Surrounding medium of neural tissues is modeled by Pasternak model. On combining these two models, 'Spherical Bidomain Pasternak-like model' is developed. The governing Partial differential equations are than solved by using the method of separation of variables. Through obtained solutions, we check the mechanical properties in actual environment of neural tissue and we compare our findings with experimental results.

2.1 Pasternak model

In the recent case the neural tissues are embedded in an elastic medium, it acts as an elastic foundation which is represented by Pasternak model. The coefficient of subgrade reaction K is the ratio among the pressure 'p' at any specified point of the surface of contact and the settlement produced by the load at that point.

There are two points, which is the basement of the Pasternak model.

1. Pasternak assumed shear interaction among the elements of spring.
2. Connecting the one end of spring to the plate or beam, which deform only in transverse shear.

$$P = KV_m - G\nabla^2 V_m \tag{1}$$

Here P is the external. potential times unit area, V_m is the potential change of the membrane, G is shearing layer potential, K is the Winkler foundation like potential and ∇ is the Laplace operator.

2.2 Bidomain tissue

We considered the tissue as a bidomain: two domains intra-cellular and extra-cellular domain having the same volume, separated by a membrane and the properties of membrane remain uniform. Due to the transmembrane current (Malmivuo and Plonsey 1995) the electric current flow from the intra-cellular region to the extra-cellular region, then the transmembrane current can be written as

$$I_m = -\nabla \cdot J_i \tag{2}$$

$$I_m = \nabla \cdot J_o \tag{3}$$

where I_m is the current in membrane, J_i and J_o are the current density for intracellular and extracellular membrane respectively.

From Ohm's law

$$J = \frac{E}{\rho} \tag{4}$$

where E is electric field strength and ρ is resistivity. Assuming that E is quasistatic. And, capacitance of tissue is full, E can be express as scalar potentials, ϕ i.e., $E = -\nabla\phi$.

For intracellular and extracellular regions E can be written as

$$E_i = -\nabla\phi_i, \quad E_o = -\nabla\phi_o$$

Using 'E' in Eq. (4) we get

$$J_i = -\frac{\nabla\phi_i}{\rho_i} \tag{5}$$

$$J_o = -\frac{\nabla\phi_o}{\rho_o} \tag{6}$$

Putting (5) and (6) in (2) and (3) respectively, then I_m can be written as

$$I_m = -\nabla.\left(-\frac{\nabla\phi_i}{\rho_i}\right) = \nabla.\left(\frac{\nabla\phi_i}{\rho_i}\right) = \frac{\nabla^2\phi_i}{\rho_i}, \quad I_m\rho_i = \nabla^2\phi_i \tag{7}$$

$$I_m = \nabla.\left(-\frac{\nabla\phi_o}{\rho_o}\right) = -\nabla.\left(\frac{\nabla\phi_o}{\rho_o}\right) = -\frac{\nabla^2\phi_o}{\rho_o}, \quad I_m\rho_o = -\nabla^2\phi_o \tag{8}$$

where the bidomain potentials, ϕ_i and ϕ_o are the potentials inside and outside of the tissue, respectively, and ρ_i and ρ_o are the intracellular and extracellular resistivity's respectively. Throughout this analysis we assume the membrane to be passive resistor which makes I_m depend upon the difference between, ϕ_i and ϕ_o

$$I_m = (\phi_i - \phi_o)\frac{\beta}{R_m} \tag{9}$$

R_m is the membrane resistance per unit area and β is the ratio between the membrane and volume of the cell.

Eqs. (7) and (8) are coupled and must be un-coupled to solve for ϕ_i and ϕ_o, by recasting the system in terms of the transmembrane potential, V_m and the mono-domain potential, ψ. In a cellular membrane the change in concentration of ions on opposite side lead a voltage is called transmembrane potential. Mathematically, the definition of V_m is

$$V_m = \phi_i - \phi_o \tag{10}$$

$$\psi = \frac{\rho_o}{\rho_i + \rho_o}\phi_i + \frac{\rho_i}{\rho_i + \rho_o}\phi_o \tag{11}$$

Then, in term of intra-and extra-cellular potential

$$V_m + \phi_o = \phi_i$$

$$\phi_i - V_m = \phi_o$$

Using these above two relations in Eq. (11), the bidomain potentials are then given as

$$\phi_i = \frac{\rho_i}{\rho_i + \rho_o}V_m + \psi \tag{12}$$

$$\phi_o = -\frac{\rho_o}{\rho_i + \rho_o}V_m + \psi \tag{13}$$

To solve for V_m, let us add Eqs. (7) and (8) and get

$$I_m\rho_i + I_m\rho_o = \nabla^2\phi_i - \nabla^2\phi_o, \quad I_m(\rho_i + \rho_o) = \nabla^2(\phi_i - \phi_o) \tag{14}$$

Using value of I_m from (9) we get

$$(\phi_i - \phi_o)\frac{\beta}{R_m}(\rho_i + \rho_o) = \nabla^2(\phi_i - \phi_o), \quad (\phi_i - \phi_o)\frac{(\rho_i + \rho_o)}{\rho_m} = \nabla^2(\phi_i - \phi_o) \tag{15}$$

where $\frac{R_m}{\beta} = \rho_m$.

Using (10) in Eq. (15) we have

$$\nabla^2 V_m - \frac{V_m}{\lambda^2} = 0 \tag{16}$$

where the length constant is, $\lambda = \sqrt{\frac{\rho_m}{\rho_i + \rho_o}}$, Eq. (16) is Helmholtz's equation.

3. Formulation of the problem

By combining the Eqs. (1) and (2) we developed spherical bidomain Pasternak-like model. The trans-membrane potential, monodomain potential and external potential can be expressed as

$$\nabla^2 V_m - \frac{V_m}{\lambda^2} = P \tag{17}$$

where the length constant is defined in Eq. (2) and P is define in Eq. (1).

$$\nabla^2 V_m - \frac{V_m}{\lambda^2} = KV_m - G\nabla^2 V_m$$

where K and G are two constant of Pasternak model.

$$\begin{aligned} &\nabla^2 V_m + G\nabla^2 V_m - KV_m - \frac{V_m}{\lambda^2} = 0 \\ &(1+G)\nabla^2 V_m - (K + \frac{1}{\lambda^2})V_m = 0 \\ &\nabla^2 V_m - \left(\frac{1 + K\lambda^2}{\lambda^2(1+G)}\right)V_m = 0 \\ &\nabla^2 V_m - \frac{T^2}{\lambda^2}V_m = 0 \end{aligned} \tag{18}$$

where $T^2 = \frac{1+K\lambda^2}{1+G}$ For monodomain and external potential equations can be written as

$$\nabla^2\psi = 0 \tag{19}$$

External to the sphere the potential, ϕ_e is given by

$$\phi_e = \phi_{bath} + \phi_{source} + \phi_{sink}$$

where ϕ_{source} and ϕ_{sink} are the fields due to the current points source and sink, respectively and are defined as

$$\phi_{source} = \frac{I_o\rho_e}{4\pi}\sum_{n=0}^{\infty}\frac{(-r)^n}{b^{n+1}}P_n(cos\,\theta)$$

$$\phi_{sink} = -\frac{I_o\rho_e}{4\pi}\sum_{n=0}^{\infty}\frac{(r)^n}{b^{n+1}}P_n(cos\,\theta)$$

ϕ_{bath} is the secondary field which also satisfies the Laplace equation

$$\nabla^2\phi_{bath} = 0 \tag{20}$$

3.1 Solution procedure

In spherical coordinates with azimuthal independence, the Laplacian operator on a function, $\nabla^2 f$ is given as

$$\nabla^2 f = \frac{1}{r^2}\frac{\partial}{\partial r}\left(r^2\frac{\partial f}{\partial r}\right) + \frac{1}{r^2\,sin\,\theta}\frac{\partial}{\partial\theta}\left(sin\,\theta\frac{\partial f}{\partial\theta}\right)$$

Then Eq. (18) can be written as

$$\frac{1}{r^2}\frac{\partial}{\partial r}\left(r^2\frac{\partial V_m}{\partial r}\right)+\frac{1}{r^2\sin\theta}\frac{\partial}{\partial\theta}\left(\sin\theta\frac{\partial V_m}{\partial\theta}\right)-\frac{T^2V_m}{\lambda^2}=0$$

This is the second order partial differential equation in r and θ. Thus, we assume a product solution of the transmembrane potential $V_m = R(r)\Theta(\theta)$, we use the method of separation of variables to get two independent, linear, ordinary and second order differential equations

$$\frac{\partial^2 R}{\partial r^2}+\frac{2}{r}\frac{\partial R}{\partial r}-\left(\frac{T^2}{\lambda^2}+\frac{\alpha}{r^2}\right)R=0 \quad (21)$$

$$\frac{\partial^2\Theta}{\partial\theta^2}+\cot\theta\frac{\partial\Theta}{\partial\theta}+\alpha\Theta=0 \quad (22)$$

where $\alpha = n(n+1)$, Eq. (21) can be transformed into modified Bessel equation by using the following transformation

$$R=\left(\frac{rT}{\lambda}\right)^{-\frac{1}{2}}P(r) \quad (23)$$

Using Eq. (23) in (21), we get

$$r^2P''(r)+rP'(r)-\left\{\left(n+\frac{1}{2}\right)+\frac{T^2r^2}{\lambda^2}\right\}\mathrm{P(r)}=0 \quad (24)$$

For the solution of above equation, we use the power series method which gives the solution in the form as

$$P(r)=AI_{n+\frac{1}{2}}\left(\frac{rT}{\lambda}\right)+BK_{n+\frac{1}{2}}\left(\frac{rT}{\lambda}\right) \quad (25)$$

Put Eq. (25) in (23), and we get

$$R(r)=\left(\frac{Tr}{\lambda}\right)^{-\frac{1}{2}}\left[AI_{n+\frac{1}{2}}\left(\frac{rT}{\lambda}\right)+BK_{n+\frac{1}{2}}\left(\frac{Tr}{\lambda}\right)\right] \quad (26)$$

Also from the Bessel identities, we have

$$I_{n+\frac{1}{2}}\left(\frac{Tr}{\lambda}\right)=\sqrt{\frac{2Tr}{\lambda\pi}}i_n\left(\frac{Tr}{\lambda}\right)\qquad K_{n+\frac{1}{2}}\left(\frac{Tr}{\lambda}\right)=\sqrt{\frac{2rT}{\lambda\pi}}k_n\left(\frac{rT}{\lambda}\right)$$

Using the above identities in Eq. (26) we have

$$R(r)=\left(\frac{Tr}{\lambda}\right)^{-\frac{1}{2}}\left[A\sqrt{\frac{T2r}{\lambda\pi}}i_n\left(\frac{rT}{\lambda}\right)+B\sqrt{\frac{2Tr}{\lambda\pi}}k_n\left(\frac{rT}{\lambda}\right)\right] \quad (27)$$

$$R(r)=A_1i_n\left(\frac{rT}{\lambda}\right)+B_1k_n\left(\frac{Tr}{\lambda}\right)$$

where $A_1=A\sqrt{\frac{2}{\pi}}$ $B_1=B\sqrt{\frac{2}{\pi}}$

Eq. (22) can be transformed to Legendre's equation and having solution

$$\Theta(\theta)=A_3P_n(\cos\theta) \quad (28)$$

where P_n is well-known Legendre polynomial having order 'n'. P_n is an nth order polynomial in θ it contains only even powers, if 'n' is even, the Rodrigues formula obviously works only for positive values of 'n' moreover it provide us one solution. The equation is second order, and it should possess two solution for every value of 'n' it turns out that these other solution blow up at the θ = 0 and or $\theta=\pi$, and unacceptable in physical grounds. In rare cases where the z-axis is for some reason inaccessible, these other solution may have to be considered.

Taking linear combination of (27) and (28), we get

$$V_m(r,\theta)=\sum_{n=0}^{\infty}\left[a_n'i_n\left(\frac{Tr}{\lambda}\right)+b_n'k_n\left(\frac{Tr}{\lambda}\right)\right]P_n(\cos\theta) \quad (29)$$

where $i_n(\frac{rT}{\lambda})$ and $k_n(\frac{Tr}{\lambda})$ are the modified spherical Bessel function of the first and second kind, respectively, of order 'n', P_n is well-known Legendre polynomial having order 'n', a_n' is the coefficient we determine from the boundary conditions, and b_n' must be zero since we need the potential to remain analytic at the origin.

$$V_m(r,\theta)=\sum_{n=0}^{\infty}a_n'i_n\left(\frac{rT}{\lambda}\right)P_n(\cos\theta) \quad (30)$$

Solution of monodomain and external potential is given by

$$\psi(r,\theta)=\sum_{n=0}^{\infty}c_n'r^nP_n(\cos\theta) \quad (31)$$

$$\phi_{bath}(r,\theta)=\sum_{n=0}^{\infty}e_n'r^{-n-1}P_n(\cos\theta) \quad (32)$$

The coefficients a_n', c_n' and e_n' which is to be determined from the boundary conditions. Now we can express transmembrane and monodomain potential in term of intra and extra-cellular potentials.

$$\phi_e=\sum_{n=0}^{\infty}e_n'r^{-n-1}P_n(\cos\theta)+\frac{I_o\rho_e}{4\pi}\sum_{n=0}^{\infty}\frac{1}{b^{n+1}}P_n(\cos\theta)\{(-r)^n-(r)^n\} \quad (33)$$

Using the values of V_m and ψ in

$$\phi_i=\frac{\rho_i}{\rho_i+\rho_o}V_m+\psi \quad \text{and} \quad \phi_o=-\frac{\rho_o}{\rho_i+\rho_o}V_m+\psi$$

we get

$$\phi_i=\frac{\rho_i}{\rho_i+\rho_o}\sum_{n=0}^{\infty}a_n'i_n\left(\frac{rT}{\lambda}\right)P_n(\cos\theta)+\sum_{n=0}^{\infty}c_n'r^nP_n(\cos\theta) \quad (34)$$

$$\phi_o=-\frac{\rho_o}{\rho_i+\rho_o}\sum_{n=0}^{\infty}a_n'i_n(\frac{Tr}{\lambda})P_n(\cos\theta)+\sum_{n=0}^{\infty}c_n'r^nP_n(\cos\theta) \quad (35)$$

The Eqs. (33), (34) and (35) are the required expression for external potential, intracellular potential and extra-cellular potential with constants, a_n', c_n' and e_n'.

3.2 Boundary Conditions

For the outer surface a resistance per unit area R_s. At the surface $r=a$ of cylinder the Ohm's law can be written as, $\phi_o(a,\theta)-\phi_e(a,\theta)=\sigma_o\frac{\partial\phi_o}{\partial r}R_s$

Where σ_o is the isotropic interstitial conductivity. For

simplicity we shall ignore the outer surface of neural tissue R_s. The three boundary conditions are defined at the tissue-bath interface, by using these conditions we will calculate the unknown coefficients a_n, c_n and e_n, are continuity of external and extracellular potentials

$$\phi_e(a,\theta) = \phi_o(a,\theta) \tag{36}$$

Continuity of normal current between bath and interstitial

$$\frac{1}{\rho_e}\frac{\partial \phi_e[r,\theta]}{\partial r}|_{r=a} = \frac{1}{\rho_o}\frac{\partial \phi_o[r,\theta]}{\partial r}|_{r=a} \tag{37}$$

And no intracellular normal current

$$\rho_i^{-1}\frac{\partial \phi_i}{\partial r}[r,\theta]|_{r=a} = 0 \tag{38}$$

Now we determine the three coefficients a_n', c_n', and e_n' for this we apply these boundary conditions on Eqs. (33), (34), and (35) we get three equations as

$$\frac{\rho_o}{\rho_i+\rho_o}\sum_{n=0}^{\infty} a_n' i_n\left(\frac{aT}{\lambda}\right) - \sum_{n=0}^{\infty} c_n' a^n + \sum_{n=0}^{\infty} e_n' a^{-n-1} + \frac{I_o\rho_e}{4\pi}\sum_{n=0}^{\infty}\frac{1}{b^{n+1}}\{(-a)^n - (a)^n\} = 0 \tag{39}$$

$$\frac{\rho_o}{\rho_i+\rho_o} a_n' i_n\left(\frac{aT}{\lambda}\right) - c_n' a^n + e_n' a^{-n-1} + \frac{I_o\rho_e}{4\pi}\frac{1}{b^{n+1}}\{(-a)^n - (a)^n\} = 0 \tag{40}$$

$$\frac{1}{\rho_i+\rho_o} a_n'\left[\frac{n}{a} i_n\left(\frac{aT}{\lambda}\right) + \frac{T}{\lambda} i_{n+1}\left(\frac{aT}{\lambda}\right)\right] - \frac{1}{\rho_o} c_n' n a^{n-1} - \frac{n+1}{\rho_e} e_n' a^{-n-2} + \frac{I_o}{4\pi}\frac{n a^{-1}}{b^{n+1}}\{(-a)^n - (a)^n\} = 0 \tag{41}$$

$$\frac{\rho_i}{\rho_i+\rho_o} a_n'\left[\frac{n}{a} i_n\left(\frac{Ta}{\lambda}\right) + \frac{T}{\lambda} i_{n+1}\left(\frac{aT}{\lambda}\right)\right] = -c_n' n a^{n-1} \tag{42}$$

Now solving the above three equations for a_n', c_n' and e_n' and we get

$$a_n' = \frac{-n\lambda(2n+1)(\rho_i+\rho_o)\rho_e\rho_o I_o\{(-a)^n - (a)^n\}}{4\pi q b^{n+1}}$$

$$c_n' = \frac{(2n+1)\rho_e I_o\rho_o\rho_i\{(-a)^n - (a)^n\}}{4\pi q b^{n+1}a^n}$$

$$e_n' = n a^{n+1}\rho_e I_o\{(-a)^n - (a)^n\}$$

$$\left[\begin{array}{l} n\lambda(\rho_i+\rho_o) i_n\left(\frac{aT}{\lambda}\right)\{\rho_e(2n^2+2n+1) - (n+1)\rho_o\} \\ + i_{n+1}\left(\frac{aT}{\lambda}\right) aT\{\rho_e(\rho_i+\rho_o)(2n^2+2n+1) - (n+1)\rho_o\rho_i\} \end{array}\right] / 4\pi q b^{n+1}(n+1)$$

where

$$q = n\lambda\{n\rho_e + (n+1)\rho_o\}(\rho_i+\rho_o) i_n\left(\frac{Ta}{\lambda}\right) + aT\{n\rho_e(\rho_i+\rho_o) + (n+1)\rho_o\rho_i\} i_{n+1}\left(\frac{aT}{\lambda}\right)$$

Completely determining all the potential fields with including elastic medium effect.

3. Results and discussions

The purpose of immersed neural tissue in elastic medium are to be analyzed and determine the electric potential difference under the effect of Pasternak parameters *G* and *K*. By comparing result with data available on the base of theoretical approach, we concluded that when *G* = 0 and *K* = 0, it shows good agreement with the results obtained from bidomain model.

Below figures show the curve for immersed neural tissue when *n* = 11, *G* = 5 *mv* and *K* = 5 *mv*. In the previous work the graphs sow the potential in free medium. Maximum potential when *G* = 0 and *K* = 0 is less than calculated by isotropic elastic bidomain model for free neural tissues. Fig. 1 shows intracellular potential which is calculated through isotropic bidomain model and the effect of elastic medium by Pasternak-like model. The values of orthotropic material constants are given in the table below.

Table 1 Represent the values of constants for neural tissue in acceptable range including Pasternak foundation parameters

Parameters name	**Symbols**	**Values**
Interstitial resistivity	ρ_i	0.19 Ωm
Intracellular resistivity	ρ_o	0.29 Ωm
Transmembrane resistivity	V_m	0.29 Ωm
Bath resistivity	ρ_e	0.15 Ωm
Interstitial point source	I_o	1.385 mA
Tissue radius	a	2 mm
Shearing layer potential	G	0-5 mV
Wrinkle constant	K	0-5 mV

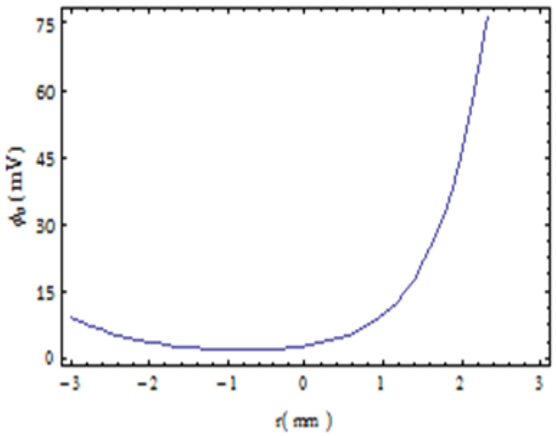

Fig. 1 Representing the relation between extracellular potential along y-axis and radius of the tissue along the x-axis also with medium effect

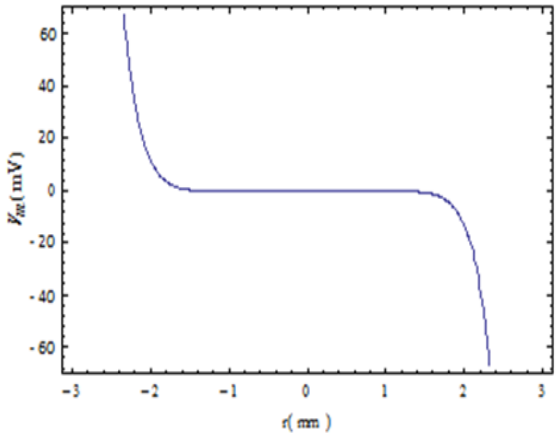

Fig. 2 Representing the relation between transmembrane potential along y-axis and radius of the tissue along the x-axis also with medium effect

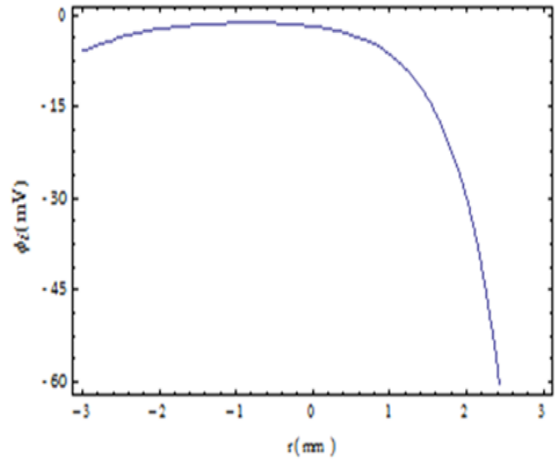

Fig. 3 Representing the relation between intracellular potential along y-axis and radius of the tissue along the x-axis also with medium effect

Declaration of conflicting interests

The author(s) declared no potential conflicts of interest with respect to the research, authorship, and/or publication of this article.

Acknowledgement

This project was supported by the Deanship of Scientific Research at Prince Sattam Bin Abdulaziz University under the research project No 16794/01/2020.

References

Altman, K.W. and Plonsey, R. (1990), "Point source nerve bundle stimulation: effects of fiber diameter and depth on simulated excitation", *IEEE T. Bio-Med. Eng.*, **37**(7), 688-698. http://doi.org/10.1109/10.55679.

Altman, K. and Plonsey, R. (1988), "Development of a model for point source electrical fibre bundle stimulation", *Med. Biol. Eng. Comput.*, **26**(5), 466-475. https://doi.org/10.1007/BF02441913.

Benmansour, D.L., Kaci, A., Bousahla, A.A., Heireche, H., Tounsi, A., Alwabli, A.S., Alhebshi, A.M., Al-ghmady, K. and Mahmoud, S.R. (2019), "The nano scale bending and dynamic properties of isolated protein microtubules based on modified strain gradient theory", *Adv. Nano Res., Int. J.*, **7**(6), 443-457. http://doi.org/10.12989/anr.2019.7.6.443.

Blochlinger, K., Bodmer, R., Jack, J., Jan, L.Y. and Jan, Y.N. (1988), "Primary structure and expression of a product from cut, a locus involved in specifying sensory organ identity in Drosophila", *Nature*, **333**(6174), 629-635. https://doi.org/10.1038/333629a0.

Bosch, B.J., Van der Zee, R., De Haan, C.A. and Rottier, P.J. (2003), "The coronavirus spike protein is a class I virus fusion protein: Structural and functional characterization of the fusion core complex", *J. Virol.*, **77**(16), 8801-8811. https://doi.org/10.1128/JVI.77.16.8801-8811.2003.

Daikh, A.A. and Zenkour, A.M. (2020), "Bending of Functionally Graded Sandwich Nanoplates Resting on Pasternak Foundation under Different Boundary Conditions", *J. Appl. Computat. Mech.*

Ebrahimi, F., Dabbagh, A., Rabczuk, T. and Tornabene, F. (2019), "Analysis of propagation characteristics of elastic waves in heterogeneous nanobeams employing a new two-step porosity-dependent homogenization scheme", *Adv. Nano Res., Int. J.*, **7**(2), 135-143. http://doi.org/10.12989/anr.2019.7.2.135.

Eltaher, M.A., Almalki, T.A., Ahmed, K.I. and Almitani, K.H. (2019), "Characterization and behaviors of single walled carbon nanotube by equivalent-continuum mechanics approach", *Adv. Nano Res., Int. J.*, **7**(1), 39-49. http://doi.org/10.12989/anr.2019.7.1.039.

Ferreira, V. (2013), "T1-mapping as a novel technique for myocardial tissue characterisation using cardiovascular magnetic resonance–from method development to clinical validation and application".

FitzHugh, R. (1969), "Mathematical models of excitation and propagation in nerve", *Biol. Eng.*, 1-85.

Hussain, M. and Selmi, A. (2020), "Effect of Pasternak foundation: Structural modal identification for vibration of FG shell", *Adv. Concrete Construct., Int. J.*, **9**(6), 569-576. https://doi.org/10.12989/acc.2020.9.6.569.

Jena, S.K., Chakraverty, S., Malikan, M. and Sedighi, H. (2020), "Implementation of Hermite–Ritz method and Navier's technique for vibration of functionally graded porous nanobeam embedded in Winkler–Pasternak elastic foundation using bi-Helmholtz nonlocal elasticity", *J. Mech. Mater. Struct.*, **15**(3), 405-434. https://doi.org/10.2140/jomms.2020.15.405.

Lee, K., Lee, S.Y., Praveenkumar, R., Kim, B., Seo, J.Y., Jeon, S.G., Jeon, S.G., Na, J.G., Park, J.Y., Kim, D.M. and Oh, Y.-K. (2014), "Repeated use of stable magnetic flocculant for efficient harvest of oleaginous Chlorella sp", *Bioresource Technol.*, **167**, 284-290. https://doi.org/10.1016/j.biortech.2014.06.055.

Liu, J., Zhang, X., Schmitter, S., Van de Moortele, P.F. and He, B. (2015), "Gradient-based electrical properties tomography (g EPT): A robust method for mapping electrical properties of biological tissues in vivo using magnetic resonance imaging", *Magn. Reson. Med.*, **74**(3), 634-646. https://doi.org/10.1002/mrm.25434.

Malmivuo, J. and Plonsey, R. (1995), *Bioelectromagnetism: Principles and Applications of Bioelectric and Biomagnetic Fields*, Oxford University Press, U.S.A.

Miller, C.E. and Henriquez, C.S. (1990), "Finite element analysis of bioelectric phenomena", *Crit. Rev. Biomed. Eng.*, **18**(3), 207-233.

Moon, P.H. and Spencer, D.E. (2013), *Foundations of Electrodynamics*, Courier Corporation.

Nicholls, J. and Purves, D. (1970), "Monosynaptic chemical and

electrical connexions between sensory and motor cells in the central nervous system of the leech", *J. Physiol*., **209**(3), 647-667. https://doi.org/10.1113/jphysiol.1970.sp009184.

Pavlović, I.R., Pavlović, R., Janevski, G., Despenić, N. and Pajković, V. (2020), "Dynamic behavior of two elastically connected NANOBEAMS under a white noise process", *Facta Universitatis, Series: Mech. Eng*., **18**(2), 219-227. https://doi.org/10.22190/FUME190415008P.

Plonsey, R. and Barr, R.C. (1984), "Current flow patterns in two-dimensional anisotropic bisyncytia with normal and extreme conductivities", *Biophys. J*., **45**(3), 557-571. https://doi.org/10.1016/S0006-3495(84)84193-4.

Plonsey, R. and Barr, R.C. (2007), *Bioelectricity: A Quantitative Approach*, Springer Science & Business Media.

Popov, V. (2020), "Coefficients of restitution in normal adhesive impact between smooth and rough elastic bodies", *Rep. Mech. Eng*., **1**(1), 103-109. https://doi.org/10.31181/rme200101103p.

Riemann, B.L. and Lephart, S.M. (2002), "The sensorimotor system, part I: the physiologic basis of functional joint stability", *J. Athletic Training*, **37**(1), 71.

Roth, S., Newman, E., Pelcovitz, D., Van Der Kolk, B. and Mandel, F.S. (1997), "Complex PTSD in victims exposed to sexual and physical abuse: Results from the DSM-IV field trial for posttraumatic stress disorder", *J. Traumatic Stress*, **10**(4), 539-555. https://doi.org/10.1023/A:1024837617768.

Sadleir, R.J., Grant, S.C. and Woo, E.J. (2010), "Can high-field MREIT be used to directly detect neural activity? Theoretical considerations", *Neuroimage*, **52**(1), 205-216. https://doi.org/10.1016/j.neuroimage.2010.04.005.

Safaei, B., Khoda, F.H. and Fattahi, A.M. (2019), "Non-classical plate model for single-layered graphene sheet for axial buckling", *Adv. Nano Res., Int. J*., **7**(4), 265-275. http://doi.org/10.12989/anr.2019.7.4.265.

Schwartz, B.L. and Sadleir, R.J. (2015), "Analysis of bipolar external excitation of spherical tissue by spatially opposed current source and sink points", *Proceedings of the 37th Annual International Conference of the IEEE Engineering in Medicine and Biology Society (EMBC)*, pp. 2299-2302, Milan, Italy, August. https://doi.org /10.1109/EMBC.2015.7318852.

Schwartz, B.L., Chauhan, M. and Sadleir, R.J. (2018), "Analytic modeling of conductively anisotropic neural tissue", *J. Appl. Phys*., **124**(6), 064701. https://doi.org/10.1063/1.5036659.

Sedighi, H.M. and Sheikhanzadeh, A. (2017), "Static and dynamic pull-in instability of nano-beams resting on elastic foundation based on the nonlocal elasticity theory", *Chinese J. Mech. Eng*., **30**(2), 385-397. https://doi.org/10.1007/s10033-017-0079-3.

Sembulingam, K. and Sembulingam, P. (2012), *Essentials of Medical Physiology*, JP Medical Ltd.

Seo, J.K. and Woo, E.J. (2011), "Magnetic resonance electrical impedance tomography (MREIT)", *SIAM Rev*., **53**(1), 40-68. https://doi.org/10.1137/080742932.

Sepulveda, N.G., Roth, B.J. and Wikswo Jr, J.P. (1989), "Current injection into a two-dimensional anisotropic bidomain", *Biophys. J*., **55**(5), 987-999. https://doi.org/10.1016/S0006-3495(89)82897-8.

Shahsavari, D., Karami, B. and Janghorban, M. (2019), "Size-dependent vibration analysis of laminated composite plates", *Adv. Nano Res., Int. J*., **7**(5), 337-349. http://doi.org/10.12989/anr.2019.7.5.337.

Sobie, E.A., Susil, R.C. and Tung, L. (1997), "A generalized activating function for predicting virtual electrodes in cardiac tissue", *Biophys. J*., **73**(3), 1410-1423. https://doi.org/10.1016/S0006-3495(97)78173-6.

Taj, M. and Zhang, J. (2012), "Analysis of vibrational behaviors of microtubules embedded within elastic medium by Pasternak model", *Biochem. Bioph. Res. Co*., **424**(1), 89-93. https://doi.org/10.1016/j.bbrc.2012.06.072.

Taj, M. and Zhang, J. (2014), "Analysis of wave propagation in orthotropic microtubules embedded within elastic medium by Pasternak model", *J. Mech. Behav. Biomed. Mater*., **30**, 300-305. https://doi.org/10.1016/j.jmbbm.2013.11.011.

Trayanova, N. (1990), "Electrical behavior of a skeletal muscle fiber in a volume conductor of finite extent", *Biol. Cybernet*., **63**(2), 121-125. https://doi.org/10.1007/BF00203034.

Trayanova, N.A., Roth, B.J. and Malden, L.J. (1993), "The response of a spherical heart to a uniform electric field: A bidomain analysis of cardiac stimulation", *IEEE T. Bio-Med. Eng*., **40**(9), 899-908. https://doi.org/10.1109/10.245611.

Weaver, J.C. (1993), "Electroporation: A general phenomenon for manipulating cells and tissues", *J. Cell. Biochem*., **51**(4), 426-435. https://doi.org/10.1002/jcb.2400510407.

Zador, A.M., Agmon-Snir, H. and Segev, I. (1995), "The morphoelectrotonic transform: A graphical approach to dendritic function", *J. Neurosci*., **15**(3), 1669-1682. https://doi.org/10.1523/JNEUROSCI.15-03-01669.1995.

JL